Nonlinear Finite Element Analysis of RC Beams without Stirrups Strengthened by Longitudinal Soffit Bonded CFRP Strips for Shear

Laith Khalid Al-Hadithy
Department of Civil Engineering/
Al-Nahrain University/ Iraq
lthadithy@yahoo.com

Mustafa Mahmood Al-Ani
National Center for Construction Laboratories
Mustafa.alani87@gmail.com

Abstract

This study concerns utilization of nonlinear finite element method for to evaluate the role of longitudinal soffit-bonded CFRP strips in elevating the shear behavior of RC beams without stirrups. All beams cross-sections were of 150 mm breadth and 200 mm depth, the overall length was 1500 mm with clear span 1300 mm. One beam was provided by minimum web reinforcement according to the ACI 318M-14, while the other five were without web reinforcement but externally strengthened by a variety of CFRP-strip combinations consisting of longitudinal soffit-bonded strips. The predictions of a proposed ANSYS (version 14.5) model for six of the test beams including modeling of concrete, steel rebars, CFRP strips and supports and loading steel plates, by SOLID65, LINK180, SHELL41 and SOLID185 elements, respectively, show high agreements with experimental evidence, which stands as a definite witness to the efficiency and reliability of the present numerical model.

Keywords: Finite Element Analysis, CFRP, Soffit-bonded, Shear resistance, Reinforced concrete beams.

Abbreviations:

RC: Reinforced Concrete
FEA: Finite Element Analysis
CFRP: Carbon Fiber Reinforced Polymer

1. Introduction

Strengthening the shear deficient RC beams by longitudinal soffit bonded CFRP strips to elevate their aptitude to withstand service lateral loads becomes profoundly necessary when their sides are not accessible to efficiently attach neither the traditional transversely aligned CFRP strips at webs nor the wrapped ones (popular in multi-girder bridge decks). Accordingly, a recent experimental study has been carried out then published to investigate the efficacy of such shear strengthening technique by CFRP strips [1].

In the respect of finite element modeling of RC beams strengthened by external CFRP strips, the onset of the third millennium attended the first development of a layered nonlinear FE model in an attempt to foretell the response of up-to-failure loaded RC beams strengthened by external CFRP strips [2], followed by several attempts in the same respects [3, 4, 5, 6, 7, 8, 9] till 2015 [10].

2. Scope and Significance

In this paper it is intended to present a comparative look between results of a finite element model prepared by employing the powerful nonlinear finite element commercial package (**ANSYS 14.5 Release**), and results of the recent experimental study published in 2016 which is identified in the preceding section (i.e. ref. No.1) by exploring the adequacy of element types, material modeling, and real constants. Results of the numerical model comprise translational displacements, normal and shear stresses in concrete, crack distribution and its propagation with progressing stages of loading and forces in longitudinal steel.

3. Description of the CFRP-Strengthened beams

In this study, the specimens are divided into two groups A and B. Group A with (a/d) equal to 3 and group B with (a/d) equal to 2.5. In fact, the presently analyzed specimens were experimentally investigated just recently by Al-Hadithy and Al-Ani [1].

Group A involves two beams strengthened by CFRP, and two reference beams. These reference beams are not strengthened by CFRP strips.

Group B involves one beam strengthened by CFRP, and one reference beams (not strengthened by CFRP).

1. Beam R1 – A: Reference beam (i.e. not strengthened with CFRP) with minimum web steel reinforcement spaced at of 85 mm on center as shown in Fig.1 which also shows the loading scheme, geometrical features and other reinforce details of reference beam R1 – A.

2. Beam R2 – A: Control beam without stirrups and not strengthened with CFRP as shown in Fig.1.

3. Beam S6 – A: Strengthened by CFRP strips installed along shear span soffit in addition to 50 mm “crooked” upward on each side of the beam "shallow U-shape shear span" 500 mm length , 250 mm width and 0.131 mm thickness each shear span. Fig. 1 shows details of beam S6 – A.

4. Beam S7 – A: Strengthened by CFRP strips installed on both sides of the beam "shallow shape" along beam 1500 mm length, 100 mm width and 0.131 mm thickness each side. Fig. 1 shows details of beam S7 – A.

5. Beam R9 – B: Control beam without stirrups and not strengthened by CFRP. Fig. 2 shows details of beam R9 - B.

6. Beam S11 – B: Strengthened by CFRP strips installed along soffit in addition to 50 mm upward on each side of the beam "shallow U-shape" 1500 mm length, 250 mm width and 0.131 mm thickness. Fig. 2 shows details of beam S11 - B.

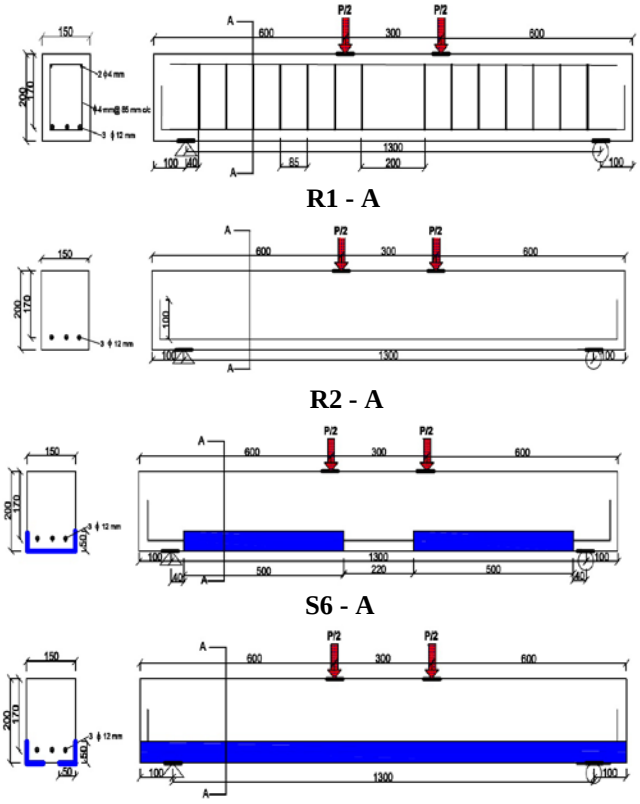

Figure 1: Beams of Group A (Al-Hadithy and Al- Ani, 2016)[1]

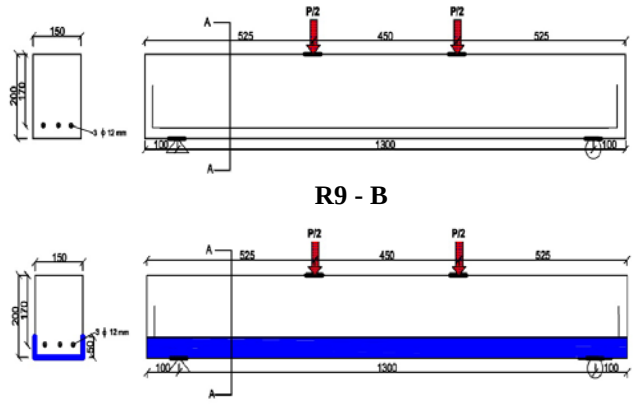

Figure 2: Beams of Group B (Al-Hadithy and Al-Ani, 2016)[1]

4. ANSYS Software and Finite Element Types

The tested beams have been modeled by the finite element method using ANSYS package (version 14.5) to investigate the accuracy of this method compared with the experimental results. In ANSYS package, Characters of the finite elements types used in modeling each of the six tested beams by ANSYS program are summarized in Table 1. Each element type in the present model has been used to represent a specified constituent of each of the six tested beams (ANSYS Manual, 2012)[11].

Table 1: Description of the used element

Beam components	Used element from ANSYS library	Element characteristics
Concrete	SOLID65	8-node Brick Element (3 translational DOF per node)
Steel reinforcing bars	LINK180	2-node Discrete Element (3 translational DOF per node)
CFRP	SHELL41	4-node shell Element (3 translational DOF and 3 rotational DOF per node)
Structural steel plate*	SOLID185	8-node Brick Element (3 translational DOF per node)

*** Used for load bearing and supports**

5. Modeling of Material Properties

5.1. Concrete

The compressive uniaxial stress-strain relationship for concrete model is obtained by using the following equations to compute the multilinear isotropic stress-strain curve for the concrete (Wolanski, 2004)[12].

Input data for the concrete properties in ANSYS computer program are introduced as follows:

a) Ultimate uniaxial compressive strength (f'c).
b) Modulus of elasticity (Ec).
c) Splitting strength of concrete (ft).
d) Poisson's ratio (ν).
e)Compressive uniaxial stress-strain relationship for concrete.
f) Shear transfer coefficient for opened and closed cracks (βo and βc respectively).

f = Ec ε/(1+(..... (1ε/(ε□²)

ε□= (2f'c/Ec) ..... (2)

Ec= (*f*/ Ɛ)..... (3)

where:
f = stress at any strain Ɛ
Ɛ = strain at stress *f*
Ɛ□= strain at ultimate compressive strength

Fig. 3 shows the simplified compressive uniaxial stress-strain relationship that was used in this study.

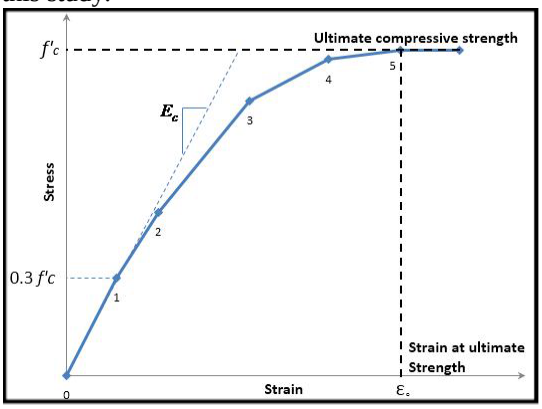

Figure 3: Simplified compressive uniaxial stress-strain curve for concrete (Bangash, 1989)[13].

The simplified stress-strain curve for each beam model is constructed from six points connected by straight lines. The curve starts at zero stress and strain. Point one at 0.30f'c, is calculated for the stress-strain relationship of the concrete in the linear range Equation 3. Points 2, 3, and 4 are obtained from Equation 1, in which Ɛ ∘ is calculated from equation 2. Point five is at Ɛ ∘ and f'c.

5.1. Steel Reinforcing Bars

The simplified bilinear stress-strain relationship shown in Fig. 4 is used in the computational process of the present ANSYS model to lessen numerical operations.

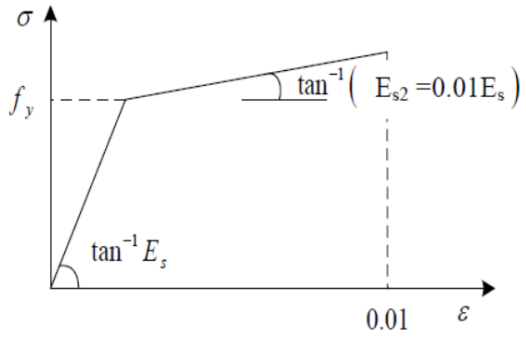

Figure 4: Idealized stress-strain relationship for computer calculations for steel.

In the present work, the modulus of strain hardening Et is taken equal to 0.01Es, an assumption necessary to avoid problems arising from divergence during iteration. On the other hand, a 0.30 value is taken for Poisson's ratio.

5.2 Structural steel plate and CFRP strips

The tensile properties of the structural steel plate (used for beneath loads and above supports) are shown in Fig.5 which also shows the membrane uni-directional tensile properties of the used CFRP strips (in the direction of fibers) for comparative purpose.

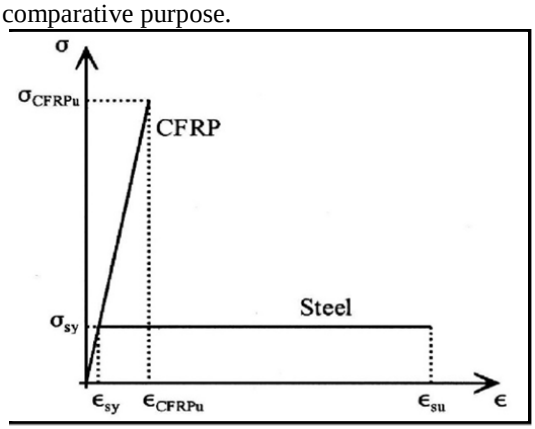

Figure 5: Comparative graph of the idealized stress-strain relationship for the structural steel plate and the CFRP.

6. Real Constants and Parameters

The main material properties included in the nonlinear material modeling of ANSYS program are drawn from standard mechanical tests. Primarily, they are the elasticity modulus, the stress versus strain relation, the yield stress and Poisson's ratio.

In the respect of selection the element type, ANSYS comprises a library for the identification of element fundamental parameters. It is of prime importance to introduce values of those parameters since the representative analogy for each modeled beam since the real constants and properties of the material are evaluated by that means. The same parameters are introduced for element LINK180, SOLID185, SHELL41 and SOLID65 are given in Table 2. However, a different parameter value is introduced for beam R1-A due to the use of 4 mm diameter steel rebars for web reinforcement as given in Table 3.

Note: three different values of the modulus of elasticity are given for the CFRP strips in the fibers direction, the orthogonal membrane direction, and the normal-to-plans direction as clarified in Table 2 below.

Table 2: Parameters of the present finite element model and their numerical values for elements LINK180, SOLID185, SHELL41 and SOLID65.

	Parameter	Definition	Value
LINK180	A_b	Area of reinforcement (mm^2) for Ø12	113
	F_y	Yield strength (MPa) for Ø12	610

	E_s	Modulus of elasticity (MPa)	200000
	E_t	Steel hardening (MPa)	2000*
	υ	Poisson's ratio	0.3*
SOLID185	Es	Modulus of elasticity (MPa)	200000*
	υ	Poisson's ratio	0.3*
SHELL41 (**)	EX	Modulus of elasticity (MPa)	234000
	EY	Modulus of elasticity (MPa)	70200*
	EZ	Modulus of elasticity (MPa)	1*
	υ	Poisson's ratio	0.3*
	t	Thickness of CFRP	0.131
SOLID65	fc'	Ultimate compressive strength (MPa)	37
	ft	Ultimate tensile strength (MPa)	3.77
	β0	Shear transfer parameters	0.3*
	βc		0.7*
	Ec	Young's modulus of elasticity (MPa)	28589
	υ	Poisson's ratio	0.2*

Definition of strain-stress relationship for concrete SOLID 65

Stress (MPa)	**0**	**2.85**	**24.88**	**32.11**	**35.82**	**37.02**
Strain	**0**	**0.0001**	**0.001**	**0.0015**	**0.002**	**0.0026**

*** Assumed values**

**** For the beams strengthened by longitudinally aligned CFRP external strips, the following values are used for modulus of elasticity of the CFRP laminates in the longitudinal, vertical and side-horizontal directions.**

Table 3: Parameter values for element LINK180 used for the 4 mm diameter steel rebars for web reinforcement in beam R1-A.

	Parameter	Definition	Value
Link180	A_b	Area of reinforcement (mm^2) for Ø4	13
	F_y	Yield strength (MPa) for Ø4	520
	E_s	Modulus of elasticity (MPa)	200000
	υ	Poisson's ratio	0.3*

*** Assumed values**

7. Modeling of Typical CFRP-Strengthened RC Beam

Due to the high adhesive strength confirmed by ref.[1], full interfering bond between CFRP strips and concrete surface is proposed. Fig. 6 shows the finite element model of strengthened beam S7-A. The high strength of the epoxy used to attach FRP strips to the experimental beams supports the perfect bond assumption.

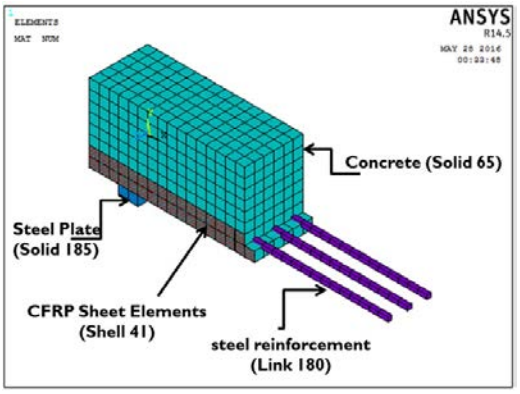

Figure 6: Modeling details of beam S7-A.

8. Meshing

In this step, the mesh generation is implemented where the results accuracy requires applying fine rectangular mesh division of the modeled beam half into a number of small-size hexahedron cubic finite element of 25 mm dimensions for their orthogonal sides. The geometrical modeling and the materials attributes for beam R1-A are shown in Fig. 7.

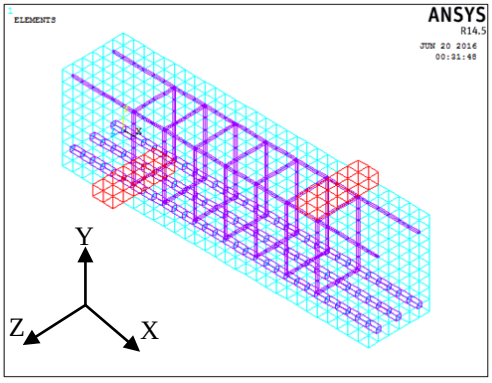

Figure 7: Element mesh and materials attributes, for beam R1-A.

9. Boundary Conditions and Applied Loads

It is necessary to impose the appropriate displacement boundary conditions to realize the proper model constraint thus controlling the rigid body motion and getting a unique solution. To guarantee that all beam models perform in a manner similar to that of the actual (i.e. physical) beam tested experimentally, a special attention has to be paid to the application of boundary conditions at locations of symmetry and those of supports and loadings. The proper locations of the planes of symmetry lie along the internal faces. In precise, rollers should be dispersed over the planes of symmetry in order to hold the displacements in the direction perpendicular to each of those planes at zero.

To provide uniform distribution of the applied external loads and the support reactions (for the sake of avoiding local crushing) steel plated of

150 x 150 x 20 mm dimensions are used beneath the applied loads and over the simple supports. The total load is then applied at the center of each loading or reaction steel plate (i.e. at 600 mm for Group A, and at 525 mm for Group B) from ridge of the beam in a manner such that it is distributed uniformly over a single transverse "nodal line" running along the breadth of the beam at its top face. Fig. 8a shows the details of boundary conditions and applied loads.

The special treatment of the supports reactions includes introducing rollers along "nodal lines" to provide the constraint of zero translation in the perpendicular direction, by that treatment, the beam rotation about that support is allowed. That support condition is shown in Fig. 8b. In the same manner, the nodes on the "nodal line" along the z-axis to provide a similar zero constraint of zero translation in the relevant perpendicular direction. Again, by that treatment the beam rotation about that support is allowed.

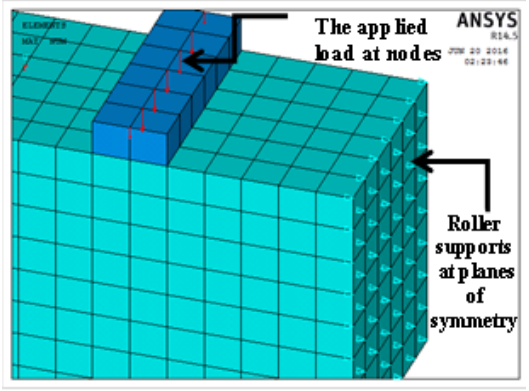

(a)

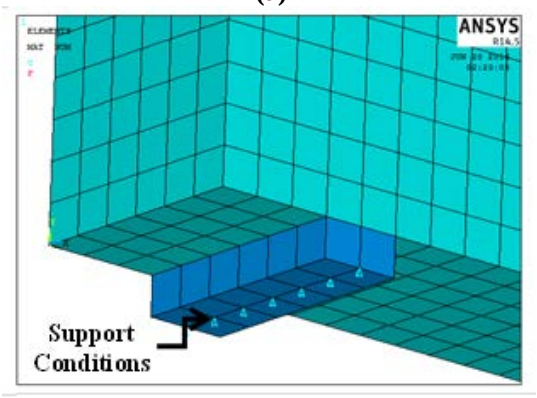

(b)

Figure 8: a) Details of boundary conditions of symmetry and applied loads, b) Details of boundary conditions of support.

10. Presentation of Results

The outputs of the ANSYS models for the six tested beams are shown in Fig. 9, where the comparative midspan load-deflection relationships for the six analyzed beam models represented load versus deflection curves are shown.

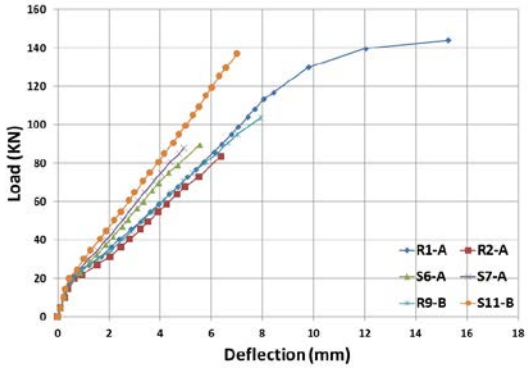

Figure 9: Comparative load versus midspan deflection relationships for the six tested beams given by the present finite element model of ANSYS program.

It is educed from Fig. 9 that the most efficient and the highest shear-strength of RC beams without steel shear reinforcement consists of "crooked" soffit-bonded strip (i.e. beam S11-B), as it gains valuable ascents in shear cracking and ultimate load.

11. Verification of the Proposed ANSYS Model

Theme:

Carried out herein is a quantitative evaluation of the efficiency and accuracy of the proposed ANSYS model by emphasizing a correlation between predictions of the present ANSYS model and the evidence of the recent experimental study [1]. In definite, precise comparisons of the curves expressing the load-deflection relations evaluated by the present numerical model and those extracted from the associated experimental investigation [1] for the seven RC beams (five of which were without internal steel stirrups, from which three were strengthened for shear by soffit bonded longitudinal CFRP strips of diverse patterns) will be discussed. Then, close insights into the patterns of fracture for the six modeled beams are presented, with a comparative inspection of the numerically determined fracture pattern and its relevant experimental one (from ref. No.1) for one the six beams will be displayed. Evaluation of the degree of reliability of the ANSYS model outcomes will be given in the following comparative respects:

i) Load versus Deflection Relationships

Results of the load versus midspan deflection relationships obtained from the present ANSYS model are compared with the experimental load versus midspan deflection ones. Good agreement can be observed in this comparison between ANSYS model results and the experimental ones presented in Figs. 10 to 15.

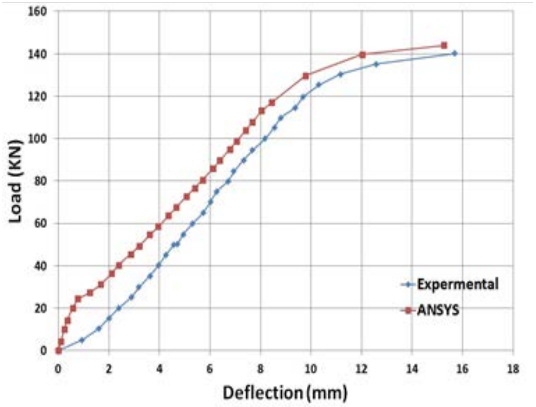

Figure 10: Load-deflection curve for beam R1-A.

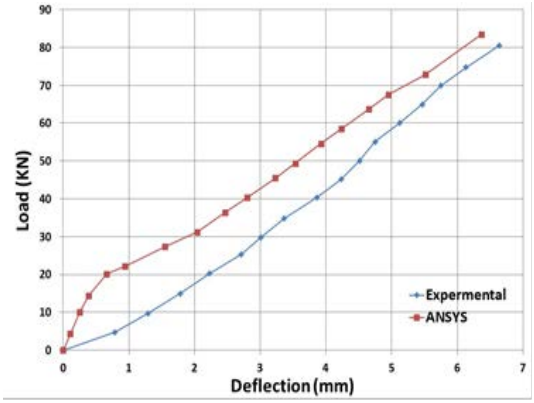

Figure 11: Load-deflection curve for beam R2-A

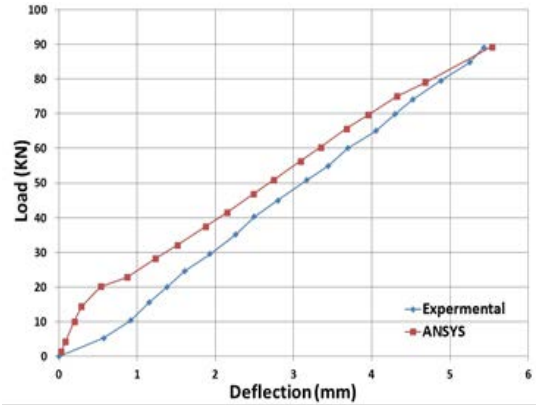

Figure 12: Load-deflection curve for beam S6-A

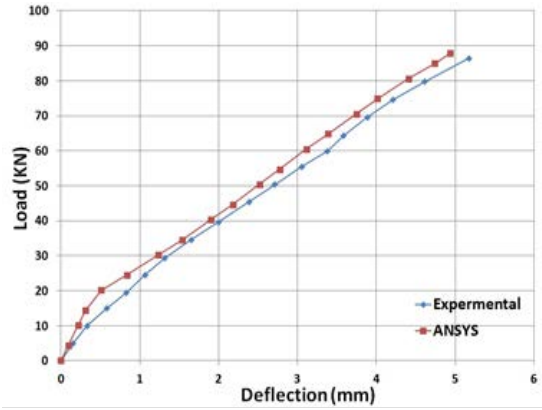

Figure 13: Load-deflection curve for beam S7-A

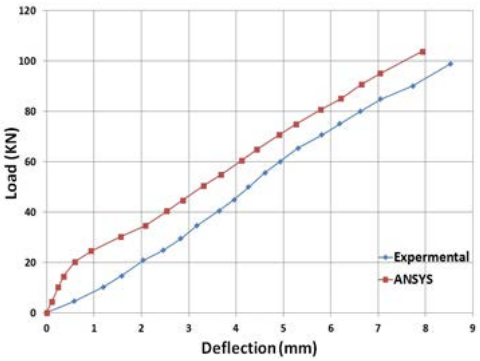

Figure 14: Load-deflection curve for beam R9-B.

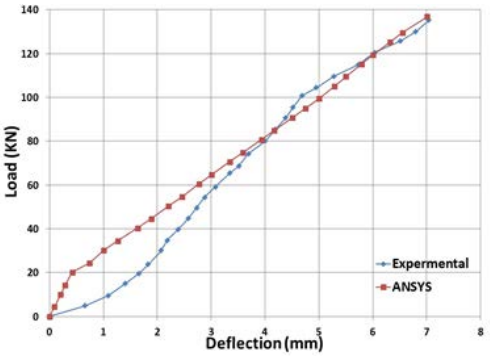

Figure 15: Load-deflection curve for beam S11-B.

ii) Agreement of Ultimate Load and Midspan Deflection Values

Close inspection of Table 4, which shows the comprehensive predication of the finite element modeling and analysis implemented by the present ANSYS model embracing a comparative look with the results extracted from the experimental investigation, it is clearly noticed that the present numerical model reveals high efficiency and reliability in the structural analysis of RC beams externally strengthened by CFRP-laminates, this assessment is based on the substantially high levels of coincidence for values of the ultimate load Pu and the midspan deflection δu given by the experimental evidence and the finite element prediction which are equal to 97.6 % and 95.6 %, respectively for the six beams comprised by the finite element analysis.

Table 4: Comparative overview on the whole prediction of the finite element analysis versus the experimental evidence.

Beam	Ultimate load p_u (kN)			Mid span deflection δ_u (mm)		
	Exp.	ANSYS	%Diff.	Exp.	ANSYS	%Diff.
R1–A*	140.1	144	2.81	15.68	15.263	2.66
R2 – A	80.50	83.52	3.75	7.07	6.368	9.93

S6 – A	89.13	89.28	0.17	5.43	5.537	1.97
S7 – A	86.40	87.84	1.67	5.17	4.936	4.53
R9 – B	98.87	103.68	4.86	8.53	7.932	7.01
S11- B	135.3	36.80	1.11	7.04	7.018	0.31
% of differenc	2.4			4.4		
Level of coincidence	97.6 %			95.6 %		

iii) Fracture Pattern at Failure

Reasonable agreements of the FE predictions for the fracture pattern of failure and those of the experimental evidence of Ref. [1] have been recognized for the six analyzed beams.

W.r.t. to Fig. 16, beam S7-A is selected have as a typical CFRP strengthened beam to view that nice agreement, represented by new features of the enhanced fracture pattern attributed to the "crook" effect and announced by the flattened outside fracture within the "crook" height.

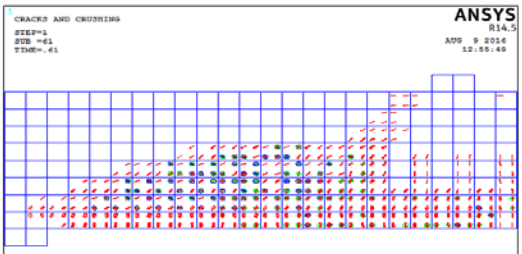

(a) Cracking pattern at failure for beam S7-A, obtained from ANSYS model

(b) Cracking pattern at failure for beam S7-A, Experimental test

Figure 16: Concrete fracture patterns at failure for beam S7-A.

The predicted fracture patterns -by the present ANSYS model- for the remaining five beams are given in Figs. 17 to 21 which reasonable fracture patterns at failure.

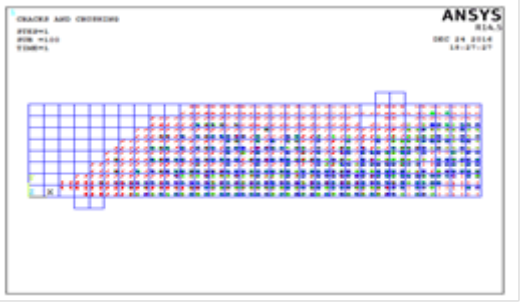

Figure 17: Cracking pattern at failure for beam R1-A, obtained from ANSYS model.

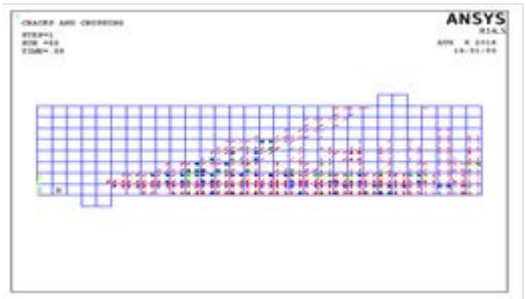

Figure 18: Cracking pattern at failure for beam R2-A, obtained from ANSYS model.

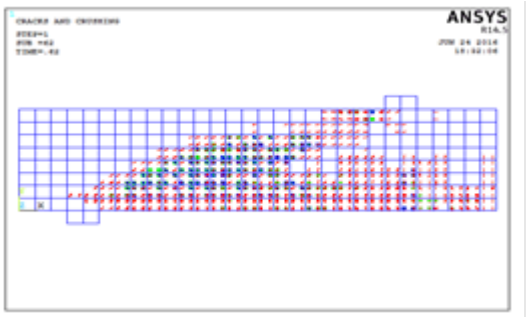

Figure 19: Cracking pattern at failure for beam S6-A, obtained from ANSYS model.

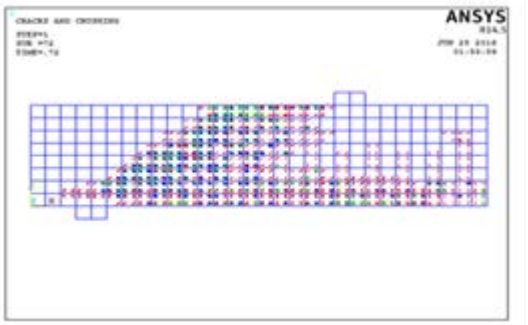

Figure 20: Cracking pattern at failure for beam R9-B, obtained from ANSYS model.

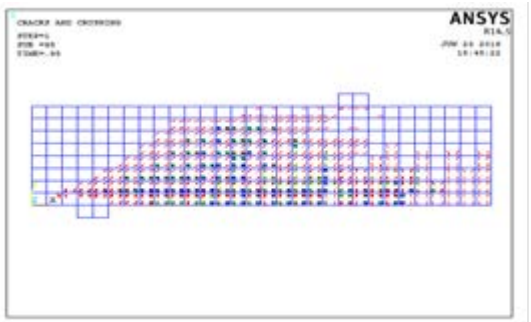

Figure 21: Cracking pattern at failure for beam S11-B, obtained from ANSYS model.

iv) Predicted Stresses in CFRP strips

Further numerical outcomes of the present ANSYS models for the three strengthened beam S6-A, S7-A and S11-B are the stresses in the CFRP strips at failure. They are all given in Figs. 22 to 24, respectively. Rational stress distributions are definitely recognized.

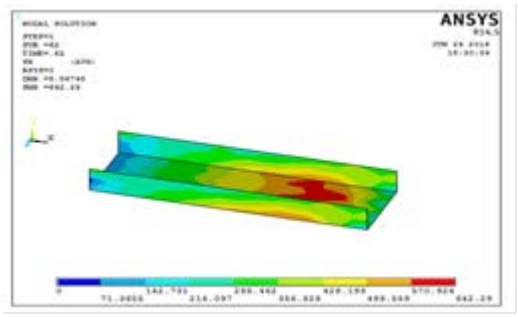

(a)

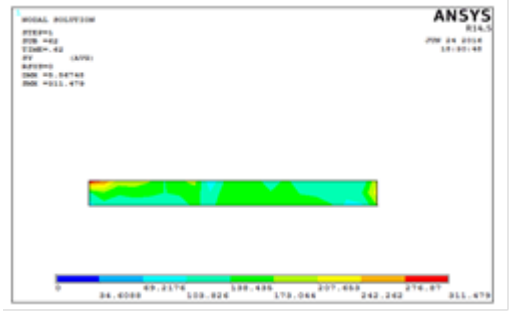

(b)

Figure 22: Maximum stress in CFRP of S6-A model obtained from ANSYS model; (a) in x-direction, (b) in y-direction.

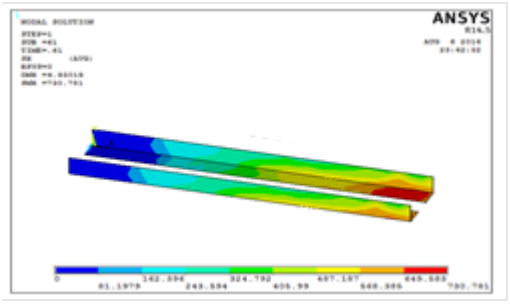

(a)

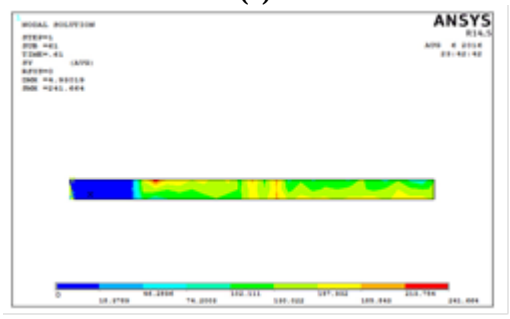

(b)

Figure 23: Maximum stress in CFRP of S7-A model obtained from ANSYS model; (a) in x-direction, (b) in y-direction.

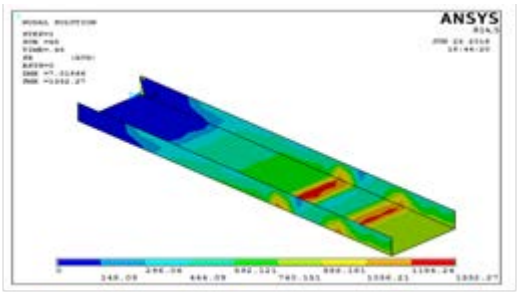

(a)

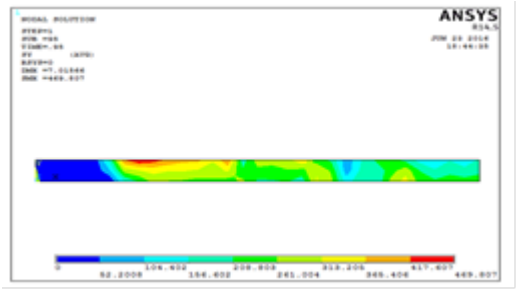

(b)

Figure 24: Maximum stress in CFRP of S11-B model obtained from ANSYS model. (a) in x-direction, (b) in y-direction.

Conclusions

From the finite element analysis the following conclusions have been drawn so far:

1. Based on comparisons predictions of the analysis by the present numerical model and the evidence of the experimental investigation for the CFRP-strengthened beams in regard to load-deflection relations, ultimate loads and accompanying deflection, the ANSYS modeled revealed high accuracy in predicting those responses as the average differences between corresponding values are 2.4 % and 4.4 % for ultimate load and deflection, respectively.
2. It has verified its reliability through its strict evaluation of the steel rebars stresses at failure of the seven modeled beams which perfectly coincides with the assumptions of the simplified plastic theory for analyzing RC beams.
3. The reason behind the decrease in value of the tensile stress in the longitudinal steel rebars of beam S7-A at failure (relative to other beams) is its early failure during loading (as predicted by ANSYS model) with load and deflection values smaller than those of other modeled CFRP-strips strengthened beams.
4. The suggested ANSYS model efficiently predicts midspan tensile stresses in the longitudinal bottom steel bars at failure of the numerically modeled beams, where the computed stress value for the reference beam R1-A (639 MPa) is the single stress exceeding the yield value of the experimentally tested steel rebars (610 MPa).
5. The significant favorite increases in values of the tensile stresses in the CFRP-laminates of

beam S11-B is attributed to its delaying failure till reaching the absolutely maximum load (of 136.8 kN value) which indicates the additional tensile stresses resisted by those laminates upto failure in comparison with the other experimentally tested and numerically investigated beams.

References

[1] Al-Hadithy, Laith Khalid and Al-Ani, Mustafa Mahmood, "Influence of Soffit Bonded CFRP Strips on Shear Capacity and Failure Type of RC Beams without Stirrups", Americans Scientific Research Journal for Engineering, Technology and Sciences (ASRJETS). 2016 Vol.26, No.4, pp. 135-150.

[2] C. Nitereka and K.W. Neale, "Analysis of Reinforced Concrete Beams Strengthened in Flexure with Composite Laminates", Canadian Journal of Civil Engineering, 1999 Vol.26, No.5, pp. 646-654.

[3] Damian I. Kachlakev, "Finite Element Analysis and Model Validation of Shear Deficient Reinforced Concrete Beams Strengthened with GFRP Laminates", California Polytechnic State, 2002.

[4] Hsuan-Teh Hu, Fu-Ming Lin, Yih-Yuan Jan, "Nonlinear Finite Element Analysis of Reinforced Concrete Beams Strengthened by Fiber-Reinforced Plastics", Composite Structures, February–March 2004 Vol.63, No.3, pp. 271-281.

[5] Al-Ta'ie, Y.M., "Nonlinear Finite Element Analysis of Reinforced Concrete Beams Strengthened with Carbon Fiber Reinforced Polymer", M.Sc. Thesis, Al-Mustansiriya University, 2006.

[6] Farhan O.S., "Shear Behavior of RC Beams Strengthened with Carbon Fiber Polymers Using Finite Element Analysis", M.Sc. Thesis, AL-Nahrain University, 2009.

[7] Majid A. Al-Jurmaa, "Non Linear Three Dimensional Finite Elements Analyses of Reinforced Concrete Beams Strengthened by CFRP", University of Mosul- College of Engineering, 2010, pp. 62-71.

[8] Amer M.I., and Mohammed SH.M., "Investigations to the Parameters Effect Shear Strength of RC Beams Strengthened with CFRP Laminations", Modern Methods and Advances in Structural Engineering and Construction, June 2011, pp.21–26.

[9] P. Jayajothi, R. Kumutha and K. Vijai, "Finite Element Analysis of FRP Strengthened RC Beams Using ANSYS", Asian Journal of Civil Engineering, February 2013 Vol. 14, No.4, pp. 631-642.

[10] Jayalin. D, Arulraj. G, Karthika.V, "Analysis of Composite Beam Using ANSYS", College of Technology, August 2015 Vol. 4, No. 9, pp. 11-15.

[11] ANSYS, 2012, "ANSYS Manual", V. 14.5 Releases.

[12] Wolanski, A. J., "Flexural Behavior of Reinforced and Prestressed Concrete Beam using Finite Element Analysis", M.Sc. Thesis, Marquette University, 2004.

[13] Bangash, M. Y. H., "Concrete and Concrete Structures: Numerical Modeling and Applications", Elsevier Science Publishers Ltd., London, England, 1989.

التحليل اللاخطي بالعناصر المحددة للعتبات الخرسانية المسلحة الخالية من الاتاري والمقوى للقص بأشرطة طولية سفلى من ألياف الكاربون البوليمرية

ليث خالد الحديثي
جامعة النهرين / قسم الهندسة المدنية

مصطفى محمود العاني
المركز الوطني للمختبرات الانشائية

الخلاصة

تعنى الدراسة الحالية باستخدام طريقة العناصر المحددة اللاخطية في تقييم تقوية سلوك القص باستخدام الاشرطة الطولية لألياف الكاربون البوليمرية الملصقة أسافل العتبات الخرسانية المسلحة الخالية من الاتاري. جميع العتبات التي تمت نمذجتها وتحليلها كانت بطول 1500 ملم، عرض 150 ملم، عمق 200 ملم وفضاء صافي 1300 ملم. وهي جميعها خالية من التسليح العرضي باستثناء عتبة واحدة مزودة بالحد الادنى من التسليح العرضي حسب متطلبات ACI 318M-14 . ان استقراءات النموذج الحالي المقترح للبرنامج ANSYS (اصدار 14.5) للعتبات الست قيد الدراسة، المتضمن نمذجة كلا من الخرسانة، قضبان التسليح، اشرطة الياف الكاربون البوليمرية والصفائح الحديدية البينية للأحمال والمساند بالعناص , SOLID65, LINK180, SHELL41 and SOLID185 اظهرت توافقاً عالياً مع النتائج التجريبية، وبذلك تكون اثباتاً مؤكداً لكفاية وموثوقية النموذج الرقمي الحالي.